

Complete set of polarization transfer coefficients for the $^3\text{He}(p, n)$ reaction at 346 MeV and 0 degrees

T. Wakasa,^{1,*} E. Ihara,¹ M. Dozono,¹ K. Hatanaka,² T. Imamura,¹ M. Kato,² S. Kuroita,¹
H. Matsubara,² T. Noro,¹ H. Okamura,² K. Sagara,¹ Y. Sakemi,³ K. Sekiguchi,⁴
K. Suda,² T. Sueta,¹ Y. Tameshige,² A. Tamii,² H. Tanabe,¹ and Y. Yamada¹

¹*Department of Physics, Kyushu University, Higashi, Fukuoka 812-8581, Japan*

²*Research Center for Nuclear Physics,*

Osaka University, Ibaraki, Osaka 567-0047, Japan

³*Cyclotron and Radioisotope Center,*

Tohoku University, Sendai, Miyagi 980-8578, Japan

⁴*RIKEN Nishina Center, Wako, Saitama 351-0198, Japan*

(Dated: October 30, 2018)

Abstract

We report measurements of the cross-section and a complete set of polarization transfer coefficients for the $^3\text{He}(p, n)$ reaction at a bombarding energy $T_p = 346$ MeV and a reaction angle $\theta_{\text{lab}} = 0^\circ$. The data are compared with the corresponding free nucleon-nucleon values on the basis of the predominance of quasi-elastic scattering processes. Significant discrepancies have been observed in the polarization transfer $D_{LL}(0^\circ)$, which are presumably the result of the three-proton $T = 3/2$ resonance. The spin-parity of the resonance is estimated to be $1/2^-$, and the distribution is consistent with previous results obtained for the same reaction at $T_p = 48.8$ MeV.

PACS numbers: 25.40.Kv, 24.70.+s, 25.10.+s

*wakasa@phys.kyushu-u.ac.jp; <http://www.kutl.kyushu-u.ac.jp/~wakasa>

I. INTRODUCTION

The search for resonances in the three-nucleon system with isospin $T = 3/2$ has a long and interesting story. Evidence for $T = 3/2$ (three-proton) resonance was found in the ${}^3\text{He}(p, n)$ reaction at the proton incident energy $T_p = 48.8$ MeV [1]. The maximum enhancement from the four-body phase space was observed at the excitation energy $E_x = 9 \pm 1$ MeV with a width $\Gamma = 10.5 \pm 1$ MeV in the three-proton system (where $E_x = 0$ at the three-proton rest mass energy). Similar enhancements have been observed for measurements at $T_p = 24.9$ MeV [2] and 197 MeV [3]. However, these studies have attributed the observed enhancements to a ${}^1\text{S}_0$ two-proton final state interaction (FSI), rather than a three-proton resonance. In the impulse approximation, the (p, n) reaction occurs only on the unpaired neutron in ${}^3\text{He}$ and the two target protons coupled to the ${}^1\text{S}_0$ state act as spectator ${}^2\text{He}$. Thus, the final state consists of three particles of p , n , and ${}^2\text{He}$, and the three-body phase space calculations reasonably explain the experimental enhancements from the four-body phase space. Therefore, the interpretation of the enhancements in the cross-section remains controversial.

Recently three-neutron $T = 3/2$ resonances have been studied in the framework of configuration-space Faddeev equations [4, 5]. Unfortunately, these studies have indicated the absence of three-neutron resonances. However, the calculations did not include three-nucleon force effects. Thus, if there exists a three-nucleon resonance with $T = 3/2$, the properties of this resonance would yield valuable information on the $T = 3/2$ three-nucleon forces [6], on which experimental data are scarce.

In this article, we present the double-differential cross-section and a complete set of polarization transfer coefficients for the ${}^3\text{He}(p, n)$ reaction at $T_p = 346$ MeV and a reaction angle $\theta_{\text{lab}} = 0^\circ$. Polarization transfer coefficients are sensitive to the spin-parity J^π of an excited state [7], and thus they are sensitive to the presence of a resonance that has a fixed J^π , as was demonstrated for the spin-dipole resonances in ${}^{12}\text{N}$ [8]. It should be noted that the polarization transfer data for the ${}^2\text{H}(p, n)$ reaction at the same incident energy and $\theta_{\text{lab}} = 0^\circ - 27^\circ$ have been well described by the free nucleon-nucleon (NN) values in the optimum frame [9, 10, 11]. Thus, comparison of the measured ${}^3\text{He}(p, n)$ data with the corresponding free NN values enables us to assess whether there exists a three-nucleon resonance. Significant differences have been observed in our data which can be interpreted as evidence for three-

proton resonance effects. The resonance properties have been discussed by comparing with distorted wave impulse approximation (DWIA) calculations.

II. EXPERIMENTAL METHODS

The data were obtained with a neutron time-of-flight (NTOF) system [12] and a neutron detector and polarimeter NPOL3 [13] at the Research Center for Nuclear Physics (RCNP), Osaka University. The experimental setup and procedure were similar to those reported previously [8, 14, 15]. Thus, in the following, we describe the detector system only briefly and discuss experimental details relevant to the present experiment.

A. Polarized proton beam

A high-intensity polarized ion source (HIPIS) at RCNP [16] was used to produce the polarized proton beam. The beam polarization direction was reversed every 5 s by selecting rf transitions in order to minimize geometrical false-asymmetries. The beam was accelerated up to $T_p = 346$ MeV by using the AVF and Ring cyclotrons. One out of seven beam pulses was selected before injecting into the Ring cyclotron, which then yielded a beam pulse period of 431 ns. This pulse selection reduces the wraparound of slow neutrons from preceding beam pulses. The single-turn extraction was maintained during the measurement in order to keep the beam polarization.

The superconducting solenoid magnets SOL1 and SOL2 located in the injection line from the AVF to Ring cyclotrons were used to precess the proton spin direction. Each magnet can rotate the direction of the polarization vector from the normal \hat{N} into sideways \hat{S} directions. These two magnets were separated by a bending angle of 45° , and the spin precession angle in this bending magnet was about 85.8° . Thus, the longitudinal (\hat{L}) and sideways (\hat{S}) polarized proton beams can be obtained at the exit of SOL2 by using the SOL1 and SOL2 magnets, respectively.

The beam polarization was continuously monitored by two sets of beam-line polarimeters, BLP1 and BLP2. These two polarimeters were separated by a bending angle of 98° , allowing simultaneous determination of all of the components of the polarization vector including the longitudinal component. Each polarimeter consists of four pairs of conjugate-angle plastic

scintillators. The $\vec{p} + p$ elastic scattering was used as the analyzing reaction, and a self-supporting CH_2 target with a thickness of 1.1 mg/cm^2 was used as the hydrogen target. The elastically scattered and recoiled protons were detected in kinematical coincidence with a pair of scintillators. The typical magnitude of the beam polarization was about 0.60.

B. ^3He target

The ^3He target was prepared as a high-pressure cooled gas target by using a target system developed for a liquid H_2 target [17]. This target was operated at temperatures down to 25 K and at absolute pressures up to 2.5 atm. Both the cell temperature and pressure were continuously monitored during the experiment, and the typical areal density was about 11 mg/cm^2 . The gas cell windows were made of $12\text{-}\mu\text{m}$ -thick Alamid foil. Background (empty-target) spectra were also measured in order to subtract the contribution from the Alamid windows. We also measured data with D_2 in the target cell at 25 and 50 K under 2.5 atm, and compared these with the data for a solid CD_2 target having a thickness of 228 mg/cm^2 . After correcting for the difference in areal density of the gaseous and solid targets, these data agreed within the systematic uncertainty associated with the areal density of the gaseous target ($\simeq 7\%$), suggesting that the performance of the gaseous target is well understood.

C. Neutron spin rotation magnet and NPOL3

A dipole magnet (NSR magnet) located at the entrance of the time-of-flight (TOF) tunnel was used to precess the neutron polarization vector from the longitudinal \hat{L}' into normal \hat{N}' directions so as to make the longitudinal component measurable with NPOL3. In the measurement of the longitudinal component of the neutron polarization, the NSR magnet was excited so that the precession angle for the neutron corresponding to the energy transfer $\omega_{\text{lab}} = 5 \text{ MeV}$ became 90° . Corrections for the over- and under-precessions to the lower and higher energy neutrons were made to account for the mixing between the longitudinal and normal components.

Neutrons were measured by the NPOL3 system [13] with a 70 m flight path length. The NPOL3 system consists of three planes of neutron detectors. The first two planes (HD1 and HD2), which act as neutron detectors and neutron polarization analyzers, are made of

20 sets of one-dimensional position-sensitive plastic scintillators (BC408) with a size of $100 \times 10 \times 5 \text{ cm}^3$. The last plane (NC), which serves as a catcher for the particles scattered by HD1 or HD2, is made of a two-dimensional position-sensitive liquid scintillator (BC519) with a size of $100 \times 100 \times 10 \text{ cm}^3$. Each of the three neutron detectors has an effective detection area of 1 m^2 .

III. DATA REDUCTION

A. Neutron detection efficiency

The neutron detection efficiency of NPOL3 (HD1 and HD2) was determined using the ${}^7\text{Li}(p, n){}^7\text{Be}(\text{g.s.} + 0.43 \text{ MeV})$ reaction at $\theta_{\text{lab}} = 0^\circ$ whose cross-section is known at $T_p = 80\text{--}795 \text{ MeV}$ [18]. The result is 0.053 ± 0.003 where the uncertainty comes mainly from the uncertainty in both the ${}^7\text{Li}$ cross-section (3%) and the thickness of the ${}^7\text{Li}$ target (3%).

B. Effective analyzing power

The neutron polarization was analyzed by using the $\vec{n} + p$ scattering in either neutron detector HD1 or HD2, and the recoiled protons were detected with neutron detector NC. The effective analyzing power $A_{y;\text{eff}}$ of NPOL3 was determined by using polarized neutrons from the Gamow–Teller (GT) ${}^2\text{H}(p, n)pp({}^1\text{S}_0)$ reaction at $T_p = 346 \text{ MeV}$ and $\theta_{\text{lab}} = 0^\circ$. We used two kinds of polarized protons with normal (p_N) and longitudinal (p_L) polarizations. The corresponding neutron polarizations at 0° become $p'_N = p_N D_{NN}(0^\circ)$ and $p'_L = p_L D_{LL}(0^\circ)$. The resulting asymmetries measured by NPOL3 are

$$\epsilon_N = p'_N A_{y;\text{eff}} = p_N D_{NN}(0^\circ) A_{y;\text{eff}} , \quad (1a)$$

$$\epsilon_L = p'_L A_{y;\text{eff}} = p_L D_{LL}(0^\circ) A_{y;\text{eff}} . \quad (1b)$$

Because the polarization transfer coefficients for the GT transition satisfy [19]

$$2D_{NN}(0^\circ) + D_{LL}(0^\circ) = -1 , \quad (2)$$

$A_{y;\text{eff}}$ can be expressed by using Eqs. (1) and (2) as

$$A_{y;\text{eff}} = - \left(2 \frac{\epsilon_N}{p_N} + \frac{\epsilon_L}{p_L} \right) . \quad (3)$$

Therefore, the $A_{y;\text{eff}}$ value can be obtained without knowing a priori the values of $D_{ii}(0^\circ)$, and the result is $A_{y;\text{eff}} = 0.130 \pm 0.004$ where the uncertainty is statistical.

The $D_{LL}(0^\circ)$ values of the $^2\text{H}(p, n)pp$ reaction at $T_p = 305\text{--}788$ MeV have been reported by McNaughton *et al.* [20]; the results are shown in Fig. 1 with open circles. The error bars represent both statistical and systematic uncertainties. The solid curve is the result of fitting with a second order polynomial. The $D_{LL}(0^\circ)$ value at $T_p = 346$ MeV, which is determined from Eq. (1b) by using the $A_{y;\text{eff}}$ value obtained, is indicated in Fig. 1 by the filled circle. Our $D_{LL}(0^\circ)$ value is consistent with the energy dependence predicted on the basis of previous data, demonstrating the reliability of our calibrations.

C. Background subtraction

Observables for the $^3\text{He}(p, n)$ reaction were extracted through a cross-section-weighted subtraction of the observables for the empty target from the observables for the full target as

$$\sigma_{^3\text{He}} = \sigma_{\text{Full}} - \sigma_{\text{Empty}} , \quad (4a)$$

$$D_{^3\text{He}} = \frac{D_{\text{Full}} - f D_{\text{Empty}}}{1 - f} , \quad (4b)$$

where σ represents the cross-section, D is one of the polarization transfer coefficients $D_{ii}(0^\circ)$, and $f = \sigma_{\text{Empty}}/\sigma_{\text{Full}}$. The fraction f was estimated by using the cross-sections based on the nominal target thicknesses and integrated beam current.

Figure 2 shows a representative set of spectra as a function of ω_{lab} . In both the full and empty target spectra, narrow peaks are observed at $\omega_{\text{lab}} = 12$ and 17 MeV and a broad bump is centered near 22 MeV. The narrow peaks result from the $^{14}\text{N}(p, n)^{14}\text{O}(2^+, 7.7 \text{ MeV})$ and $^{12}\text{C}(p, n)^{12}\text{N}(1^+, \text{g.s.})$ reactions on the Alamid windows. The broad bump is mainly due to the spin-dipole resonances in ^{12}N excited by the (p, n) reaction on ^{12}C in Alamid. The signal-to-background ratio, integrated up to $\omega_{\text{lab}} = 50$ MeV, is about 1.3, which is significantly better than that obtained in the previous experiment (0.17) at $T_p = 197$ MeV [3]. This is mainly thanks to the use of the relatively thin Alamid foil for the target windows.

The filled histogram in Fig. 2 shows the subtraction results. The background contributions including narrow peaks and the broad bump are successfully subtracted without adjusting the relative normalization, demonstrating the reliability of our measurements.

The vertical dashed line represents the energy transfer for the three-proton rest system. Because there is no bound state in the three-proton system, the spectrum of the ${}^3\text{He}(p, n)$ reaction shows a rise due to this energy transfer.

IV. RESULTS

Figure 3 shows the double-differential cross-section I and the complete set of polarization transfer coefficients $D_{NN}(0^\circ)$ and $D_{LL}(0^\circ)$ for the ${}^3\text{He}(p, n)$ reaction at $T_p = 346$ MeV and $\theta_{\text{lab}} = 0^\circ$. The data for the cross-section are binned in 1 MeV intervals, while the data for $D_{ii}(0^\circ)$ are binned in 2 MeV intervals to reduce statistical fluctuations. The slope of the cross-section spectrum near the threshold is primarily determined by the phase space factor, and is consistent with that at $T_p = 197$ MeV [3]. Palarczyk *et al.* [3] reported phase-space calculations and showed that the increase in cross-section near the threshold is reproduced better by three-body than four-body phase space calculations. This means that the present ${}^3\text{He}(p, n)$ reaction can be described by $n(p, n)p$ quasi-elastic scattering on the neutron in ${}^3\text{He}$, whereas the two protons in the relative ${}^1\text{S}_0$ state act as a spectator. Thus, the measured polarization transfer coefficients are expected to be well described by the corresponding free NN values.

The dashed curves in Fig. 3 represent the corresponding free NN values with the FA07 phase-shift solution [21] of the on-line Scattering Analysis Interactive Dial-in (SAID) Facility [22]. The uncertainty in the free NN values was evaluated by using the modern nucleon-nucleon NN potentials of AV18 [23], CD Bonn [24], Nijmegen 93 [25], and Paris [26]. The results are represented in Fig. 3 by the shaded bands. The measured $D_{NN}(0^\circ)$ values are close to the corresponding free NN values. This supports the predominance of quasi-elastic scattering processes in this reaction. However, significant discrepancies are observed in $D_{LL}(0^\circ)$. The discrepancies at $\omega_{\text{lab}} \gtrsim 30$ MeV might be due to the energy dependence of $A_{y;\text{eff}}$ which was neglected in the present analysis.

The present analysis was based on the assumption of simple quasi-elastic scattering, and thus the discrepancies at $\omega_{\text{lab}} \lesssim 30$ MeV do not necessarily evidence $T = 3/2$ three-proton resonance. One possibility is the effects of the D -state in ${}^3\text{He}$. The deuteron D -state effects for ${}^2\text{H}(p, n)$ at the same incident energy were studied by Sakai *et al.* [9] using the plane wave impulse approximation code developed by Itabashi *et al.* [27]. They concluded that

the effects to the cross section at $\theta_{\text{lab}} = 0^\circ$ are negligible at small energy transfers where the $^1\text{S}_0$ FSI process is dominant. We performed the calculations using the same code in order to investigate the D -state effects to the polarization transfer coefficients at energy transfers up to 50 MeV. The D -state contributions to the cross section become appreciable beyond the FSI region as increasing the energy transfer. However, their effects to the polarization transfer coefficients are very small, namely, less than 0.04 at $\omega_{\text{lab}} < 50$ MeV. Therefore, we expect that the D -state effects to $D_{NN}(0^\circ)$ and $D_{LL}(0^\circ)$ for $^3\text{He}(p, n)$ are also small, and thus it is interesting to investigate the discrepancies by assuming the effects due to the $T = 3/2$ three-proton resonance contribution. In the following, we performed DWIA calculations in order to determine the J^π and strength of the resonance.

V. DISCUSSION

A. DWIA calculations

We performed full microscopic DWIA calculations by using the computer code DW81 [28], which treats the knock-on exchange amplitude exactly. The final states with $J^\pi = 1/2^\pm$ and $3/2^\pm$ were investigated [5]. The one-body density matrix elements for the transitions to these states by $^3\text{He}(p, n)$ were obtained with the shell-model (SM) code OXBASH [29]. The SM calculations were performed in the $0s\text{-}0p\text{-}1s0d\text{-}0f1p$ configuration space by using the phenomenological effective interaction optimized for $A=3$ by Hosaka, Kubo, and Toki [30]. For each transition, only the lowest-energy state was investigated by DWIA calculations because the $D_{ii}(0^\circ)$ values are primarily determined by J^π [7]. The single-particle radial wave functions were assumed to have a harmonic oscillator shape with the range parameter $b = 1.67$ fm [31]. The optical model potential (OMP) was deduced from the global OMPs optimized for ^4He in the proton energy range $T_p = 156\text{--}1728$ MeV [32]. The NN t -matrix parameterized by Franey and Love at 325 MeV [33] was used.

The DWIA calculation results are summarized in Table I. In order to reproduce the observed $D_{ii}(0^\circ)$ values, the $D_{NN}(0^\circ)$ value of the resonance should be close to the observed value of ~ -0.2 , whereas the $D_{LL}(0^\circ)$ value should be significantly larger than the observed value of ~ -0.3 . This constraint is satisfied only in the case of $J^\pi = 1/2^-$. Thus, in the following, we deduce the strength distribution of the resonance by assuming $J^\pi = 1/2^-$.

B. Resonance contributions

Here we assume that the observed ${}^3\text{He}(p, n)$ cross-section comprises an incoherent sum of contributions from quasi-elastic scattering and the resonance with $J^\pi = 1/2^-$. Thus, the observed $D_{ii}(0^\circ)$ values can be expressed by using the observed cross-section $\sigma(0^\circ)$ as

$$D_{NN}(0^\circ) = \frac{\sigma^{1/2^-}(0^\circ)D_{NN}^{1/2^-}(0^\circ) + (\sigma(0^\circ) - \sigma^{1/2^-}(0^\circ))D_{NN}^{\text{QES}}(0^\circ)}{\sigma(0^\circ)}, \quad (5a)$$

$$D_{LL}(0^\circ) = \frac{\sigma^{1/2^-}(0^\circ)D_{LL}^{1/2^-}(0^\circ) + (\sigma(0^\circ) - \sigma^{1/2^-}(0^\circ))D_{LL}^{\text{QES}}(0^\circ)}{\sigma(0^\circ)}, \quad (5b)$$

where $D_{ii}^{1/2^-}(0^\circ)$ and $D_{ii}^{\text{QES}}(0^\circ)$ are the $D_{ii}(0^\circ)$ values for the resonance with $J^\pi = 1/2^-$ and the quasi-elastic scattering (free NN scattering), respectively, and $\sigma^{1/2^-}$ is the cross-section of the resonance. The shape of $\sigma^{1/2^-}$ is described by a Bright–Wigner (Lorentz) function, and threshold (phase-space) effects are taken into account. The center ω_0 , width Γ (full width at half maximum), and amplitude of $\sigma^{1/2^-}$ are determined to satisfy Eq. (5) by using the $D_{ii}^{1/2^-}(0^\circ)$ and $D_{ii}^{\text{QES}}(0^\circ)$ values evaluated from the DWIA calculations and free NN values, respectively.

The thick and thin lines in Fig. 4 show the results of fitting for $\omega_{\text{lab}} < 30$ and 50 MeV, respectively. The solid histograms and curves in the top panel represent the $\sigma^{1/2^-}$ values. The solid histograms in the lower two panels are the $D_{ii}(0^\circ)$ values evaluated by Eq. (5). The shaded bands represent the errors of the fitting results for $\omega_{\text{lab}} < 30$ MeV due to the uncertainty of the experimental data. The dashed curves show the $D_{ii}^{\text{QES}}(0^\circ)$ values of the quasi-elastic scattering contribution. By considering the contributions from $J^\pi = 1/2^-$, both the $D_{NN}(0^\circ)$ and $D_{LL}(0^\circ)$ values are well reproduced.

The center of $\sigma^{1/2^-}$ is almost independent of the fitting region, and the results are $\omega_0 = 16 \pm 1$ and 17 ± 1 MeV for the fitting regions of $\omega_{\text{lab}} < 30$ and 50 MeV, respectively. However, the width depends on the fitting region and the results are $\Gamma = 11 \pm 3$ and 19 ± 6 MeV for $\omega_{\text{lab}} < 30$ and 50 MeV, respectively. In the case of $\omega_{\text{lab}} < 50$ MeV, the large Γ value of 19 MeV makes it difficult to interpret this contribution as a resonance. On the contrary, if we adopt the results for $\omega_{\text{lab}} < 30$ MeV where the systematic uncertainties of the data coming from the energy dependence of $A_{y;\text{eff}}$ are small, the interpretation as a resonance is reasonable due to the relatively narrow width of 11 MeV. If we choose the excitation energy $E_x = 0$ of the three-proton system to be at the three-proton rest mass energy, $\omega_0 = 16$ MeV corresponds

to $E_x = 10$ MeV. Thus, it is very interesting to note that our results are consistent with the results of $E_x = 9 \pm 1$ MeV and $\Gamma = 10.5 \pm 1$ MeV for a possible $T = 3/2$ resonance observed by the same reaction [1]. Because the present analyses have been based on the simple quasi-elastic scattering mechanism, detailed theoretical investigations are highly required in order to confirm the discrepancies observed in $D_{LL}(0^\circ)$ as the three-proton resonance effects.

VI. SUMMARY AND CONCLUSION

The cross-section and a complete set of polarization transfer coefficients were measured for the ${}^3\text{He}(p, n)$ reaction at $T_p = 346$ MeV and $\theta_{\text{lab}} = 0^\circ$. The data are compared with the corresponding free NN values under the assumption that the quasi-elastic scattering processes are predominant. Significant deviations were observed from the corresponding NN values in the polarization transfer $D_{LL}(0^\circ)$. These discrepancies can be attributed to the three-nucleon $T = 3/2$ resonance whose spin-parity J^π is estimated to be $1/2^-$ in DWIA calculations. The center ω_0 and the width Γ of the resonance are estimated to be $\omega_0 = 16 \pm 1$ MeV and $\Gamma = 11 \pm 3$ MeV by using the data at $\omega_{\text{lab}} < 30$ MeV whose systematic uncertainties are small. The estimated strength distribution is consistent with previous results obtained from the same reaction at $T_p = 48.8$ MeV. However, the present data are not conclusive evidence for the three-nucleon resonance, and call for the theoretical calculation which incorporates the Coulomb interaction and the $T = 3/2$ three-nucleon forces in order to settle the interpretation of the present data.

Acknowledgments

We are grateful to Professor M. Ichimura for his helpful correspondence. We also acknowledge the dedicated efforts of the RCNP cyclotron crew for providing a high quality polarized proton beam. The experiment was performed at RCNP under Program Number E300. This research was supported in part by the Ministry of Education, Culture, Sports, Science, and Technology of Japan.

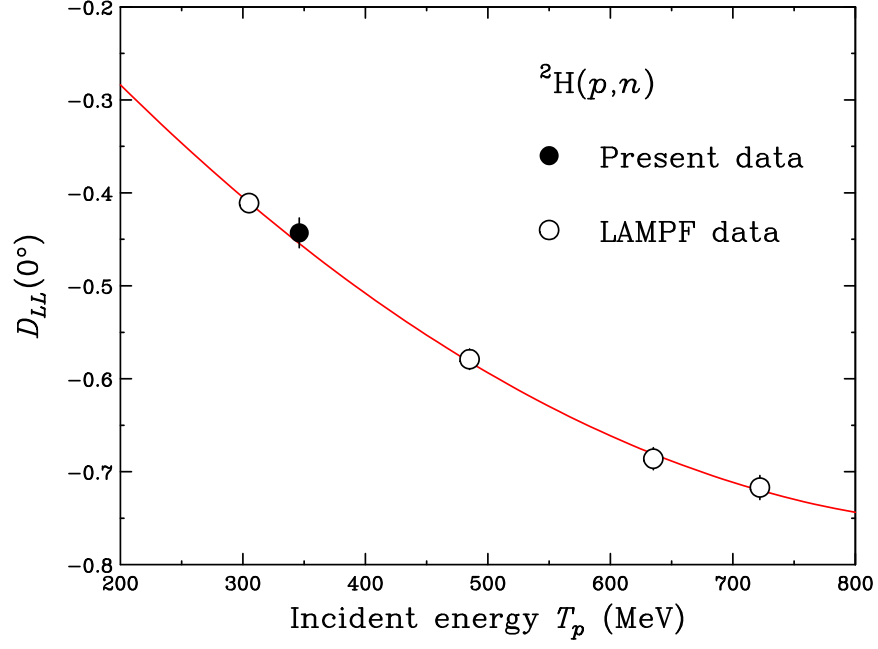


FIG. 1: (Color online) Polarization transfer $D_{LL}(0^\circ)$ for the ${}^2\text{H}(p,n)$ reaction at 0° as a function of incident energy T_p . The filled circle is the present result, while the open circles show the data by McNaughton *et al.* [20]. The solid curve represents the fit with a second order polynomial.

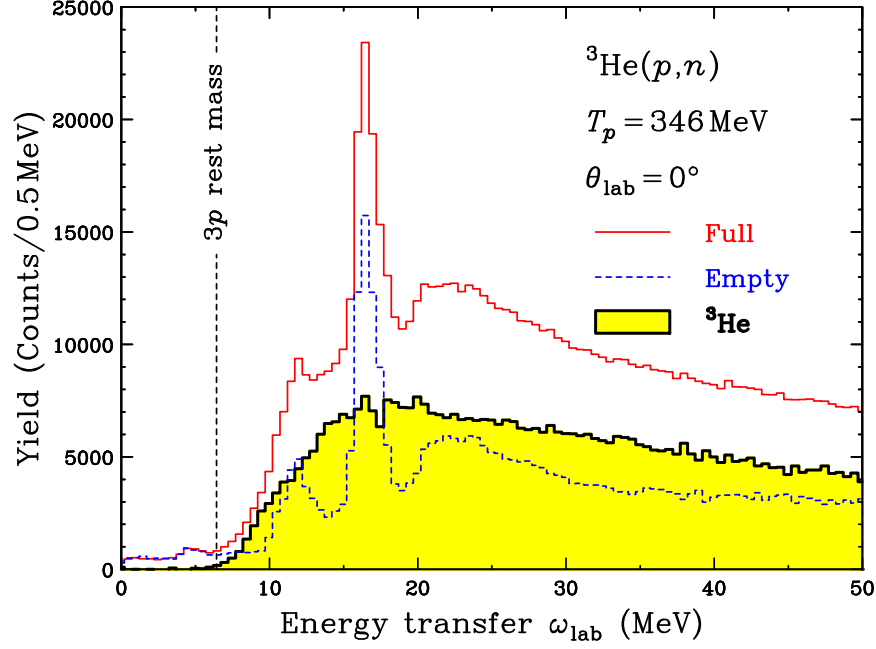


FIG. 2: (Color online) Energy transfer spectra with an empty target (dashed histogram) and a target filled with ${}^3\text{He}$ gas (thin-solid histogram) for the (p,n) reaction at $T_p = 346 \text{ MeV}$ and $\theta_{\text{lab}} = 0^\circ$. The narrow peaks are from (p,n) reactions on the elements of the Alamid windows. The filled thick-solid histogram shows the spectra for the ${}^3\text{He}(p,n)$ reaction obtained by the subtraction of Eq. (4).

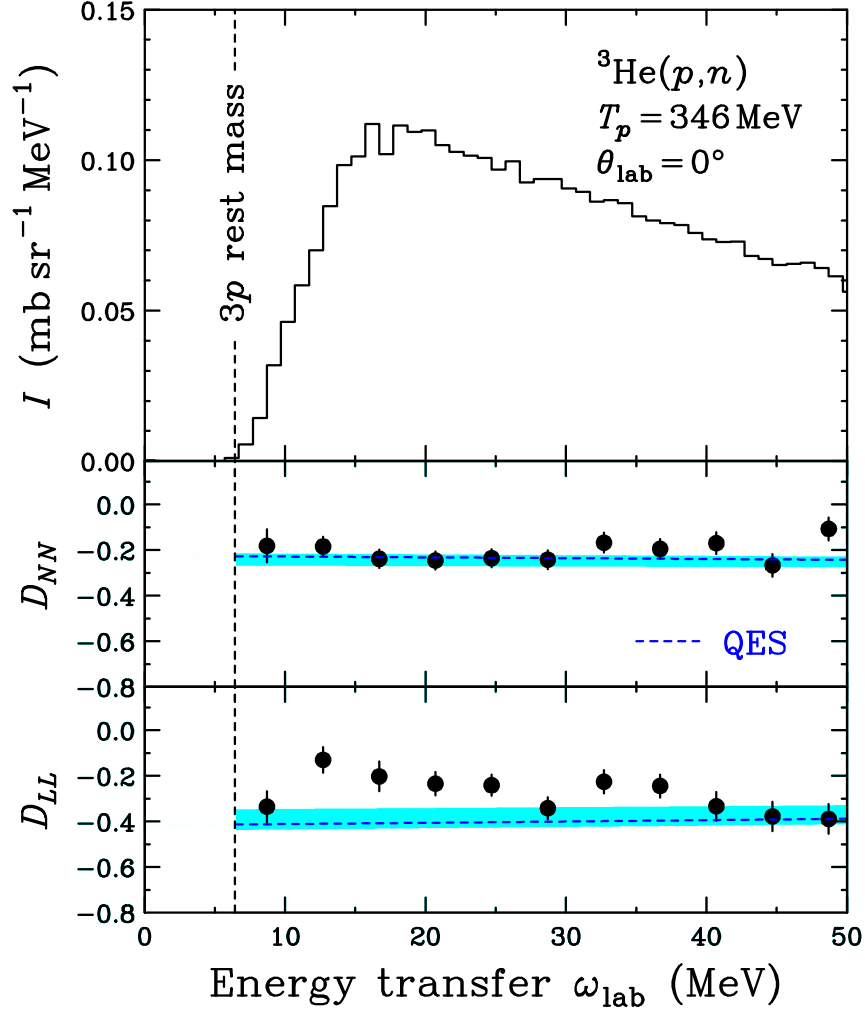


FIG. 3: (Color online) The double-differential cross-section I (top panel) and complete set of polarization transfer coefficients, $D_{NN}(0^\circ)$ (middle panel) and $D_{LL}(0^\circ)$ (bottom panel), for the ${}^3\text{He}(p, n)$ reaction at $T_p = 346$ MeV and $\theta_{\text{lab}} = 0^\circ$. The dashed curves are the corresponding free NN values with the FA07 phase-shift solution [21]. The shaded bands represent the uncertainty in the free NN values estimated by using the up-to-date NN potentials, as described in the text.

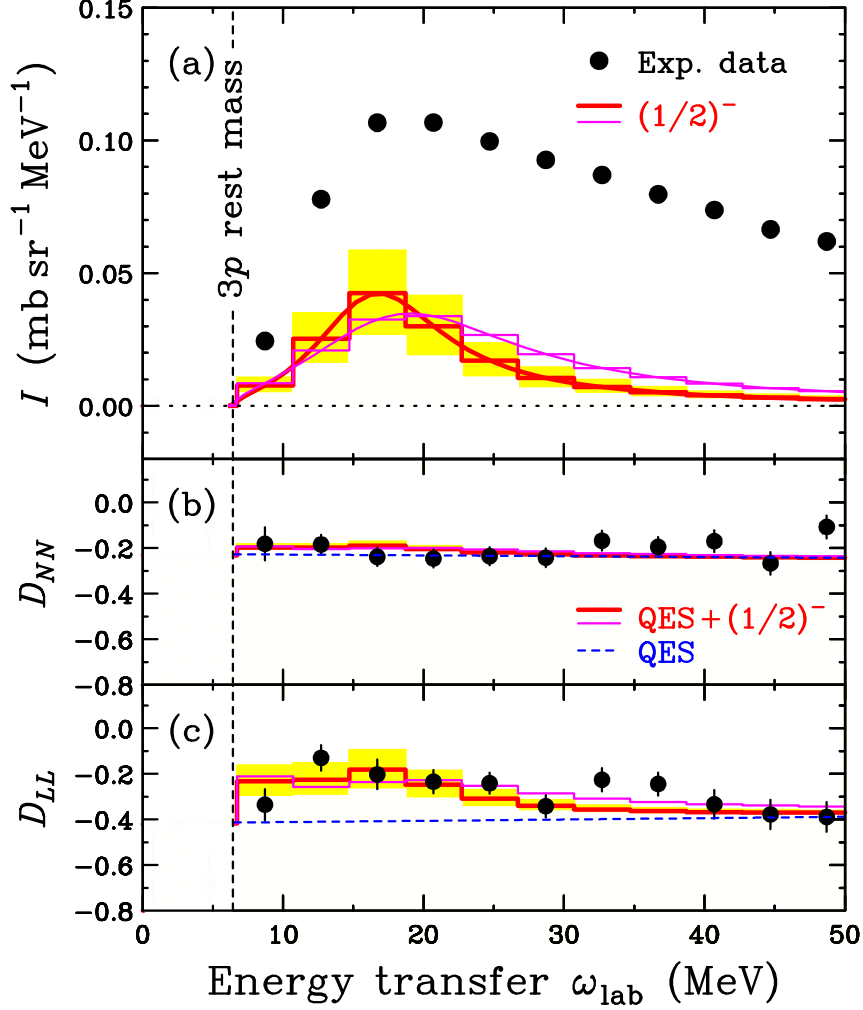


FIG. 4: (Color online) (a) The estimated $J^\pi = 1/2^-$ $T = 3/2$ resonance cross-section (solid histograms and curves) compared with the total cross-section (filled circles) for the $^3\text{He}(p, n)$ reaction at $T_p = 346$ MeV and $\theta_{\text{lab}} = 0^\circ$. The thick and thin lines are the results of fitting for $\omega_{\text{lab}} < 30$ and 50 MeV, respectively. (b) The $D_{NN}(0^\circ)$ values including the $J^\pi = 1/2^-$ resonance contributions with Eq. (5) (solid histogram) compared with the experimental data (filled circles). The band represents the uncertainty of the fitting for $\omega_{\text{lab}} < 30$ MeV due to the uncertainty of the experimental data. The dashed curve represents the corresponding free NN values with the FA07 phase-shift solution [21]. (c) Same as (b), but for $D_{LL}(0^\circ)$.

TABLE I: DWIA predictions of the polarization transfer coefficients $D_{NN}(0^\circ)$ and $D_{LL}(0^\circ)$ for the ${}^3\text{He}(p, n)3p$ reaction at $T_p=346$ MeV and $\theta_{\text{lab}}=0^\circ$.

J^π	$D_{NN}(0^\circ)$	$D_{LL}(0^\circ)$
$1/2^+$	-0.17	-0.56
$1/2^-$	-0.11	0.18
$3/2^+$	-0.15	-0.65
$3/2^-$	0.16	-0.33

-
- [1] L. E. Williams, C. J. Batty, B. E. Bonner, C. Tschalär, H. C. Benöhr, and A. S. Clouth, Phys. Rev. Lett. **23**, 1181 (1969).
- [2] A. D. Bacher, F. G. Resmini, R. J. Slobodrian, R. D. Swiniarski, H. Heimer, and W. M. Tivol, Phys. Lett. B **29**, 573 (1969).
- [3] M. Palarczyk et al., Phys. Rev. C **58**, 645 (1998).
- [4] H. Witała and W. Glöckle, Phys. Rev. C **60**, 024002 (1999).
- [5] A. Hemmdan, W. Glöckle, and H. Kamada, Phys. Rev. C **66**, 054001 (2002).
- [6] S. C. Pieper, V. R. Pandharipande, R. B. Wiringa, and J. Carlson, Phys. Rev. C **64**, 014001 (2001).
- [7] J. M. Moss, Phys. Rev. C **26**, 727 (1982).
- [8] M. Dozono et al., J. Phys. Soc. Jpn. **77**, 014201 (2008).
- [9] H. Sakai et al., Nucl. Phys. A **631**, 757c (1998).
- [10] T. Wakasa et al., Phys. Rev. C **59**, 3177 (1999).
- [11] T. Wakasa et al., Phys. Rev. C **69**, 044602 (2004).
- [12] H. Sakai, H. Okamura, H. Otsu, T. Wakasa, S. Ishida, N. Sakamoto, T. Uesaka, Y. Satou, S. Fujita, and K. Hatanaka, Nucl. Instrum. Methods Phys. Res. A **369**, 120 (1996).
- [13] T. Wakasa et al., Nucl. Instrum. Methods Phys. Res. A **547**, 569 (2005).
- [14] T. Wakasa et al., Phys. Lett. B **645**, 402 (2007).
- [15] T. Wakasa et al., Phys. Lett. B **656**, 38 (2007).
- [16] K. Hatanaka, K. Takahisa, H. Tamura, M. Sato, and I. Miura, Nucl. Instrum. Methods Phys. Res. A **384**, 575 (1997).
- [17] T. Yagita et al., Mod. Phys. Lett. A **18**, 322 (2003).
- [18] T. N. Taddeucci et al., Phys. Rev. C **41**, 2548 (1990).
- [19] T. Wakasa et al., J. Phys. Soc. Jpn. **73**, 1611 (2004).
- [20] M. W. McNaughton et al., Phys. Rev. C **45**, 2564 (1992).
- [21] R. A. Arndt, W. J. Briscoe, I. I. Strakovsky, and R. L. Workman, Phys. Rev. C **76**, 025209 (2007).
- [22] <http://gwdac.phys.gwu.edu/>.
- [23] R. B. Wiringa, V. G. J. Stoks, and R. Schiavilla, Phys. Rev. C **51**, 38 (1995).

- [24] R. Machleidt, Phys. Rev. C **63**, 024001 (2001).
- [25] V. G. J. Stoks, R. A. M. Klomp, C. P. F. Terheggen, and J. J. de Swart, Phys. Rev. C **49**, 2950 (1994).
- [26] M. Lacombe, B. Loiseau, J. M. Richard, R. V. Mau, J. Côté, P. Pirés, and R. de Tournell, Phys. Rev. C **21**, 861 (1980).
- [27] A. Itabashi, K. Aizawa, and M. Ichimura, Prog. Theor. Phys. **91**, 69 (1994).
- [28] R. Schaeffer and J. Raynal, Program DW70 (unpublished); J. Raynal, Nucl. Phys. A **97**, 572 (1967); J. R. Comfort, Extended version DW81 (unpublished).
- [29] B. A. Brown, A. Etchegoyen, W. D. M. Rae, N. S. Godwin, W. A. Richter, C. H. Zimmerman, W. E. Ormand, and J. S. Winfield, MSU-NSCL Report No. 524, 1985 (unpublished).
- [30] A. Hosaka, K.-I. Kubo, and H. Toki, Nucl. Phys. A **444**, 76 (1985).
- [31] D. Halderson, M. Yu, and J. Yu, Phys. Rev. C **39**, 336 (1989).
- [32] B. C. Clark, E. D. Cooper, and S. Hama, Phys. Rev. C **73**, 024608 (2006).
- [33] M. A. Franey and W. G. Love, Phys. Rev. C **31**, 488 (1985).